Chapter 2

ATP CONSUMPTION IN SPACE AND TIME IN MICROTUBULE-MOTOR STRUCTURES

2.1 Abstract

Living matter produces a variety of beautiful spatiotemporal structures and patterns that are not present in their nonliving counterparts. Often, these ordered, non-equilibrium steady states are sustained through the consumption of energy. Careful examination of when and where living systems direct energy consumption helps us understand the principles dictating such ordering and can motivate development of non-equilibrium theories that apply to living matter. Here, we investigate the energetic cost of assembling an ordered aster from a disordered, uniform mixture of cytoskeletal microtubules and kinesin motors. Using a fluorescent ATP sensor, we perform a careful measurement of ATP consumption through space and time on an in vitro cytoskeletal network. Our experiments resolve the emergence of radial ATP gradients. We successfully predict how a given motor profile generates these ATP distributions using reaction-diffusion models in conjunction with finite element simulations. With our results, we compare the power per volume required by our cytoskeletal networks with the known power per volume expenditure in cells, leading to the hypothesis that one of the primary energy drains in the context of these systems is the production and maintenance of spatial motor gradients. Our direct quantification of energetic fluxes across space unlocks future explorations of what steady states are accessible to cells, and how the cytoskeleton drives broad spatial organization.

2.2 Introduction

One of the main drivers maintaining the rich patterns in living matter is a steady investment of energy. For example, the existence of morphogen gradients in developmental patterning is paid for through a steady flux of protein synthesis and degradation. Similarly, cytoskeletal-motor systems hydrolyze ATP and GTP to achieve processes ranging from intracellular transport, to cell motility, to chromosome segregation. Motivated by these processes, we were inspired to develop a physical understanding of the connection between energy fluxes and the emergence of biological order in space and time in the context of the particular example of

microtubule-motor assemblies.

The energetic basis of the processes within living cells are based upon a few fundamental energy currencies, which can be thought of as a sort of biological batteries. This metaphor is useful because it reminds us that batteries are indifferent to the particulars of what they are wired up to – they can drive anything from the light in a flashlight to motorized toys. Biological processes are powered by several key biological batteries including membrane potentials, redox reactions and trinucleotide hydrolysis. Indeed, for the molecular motor driven reactions that power the structures of the cytoskeleton, ATP and GTP hydrolysis are central. Thus, we were curious about how ATP consumption in space and time drives the dynamics of structure formation.

Recently, it has become possible to measure the total energy consumption of both living organisms and the molecular machinery that drive them [1, 2, 3, 4]. We aimed to complement these foundational studies by investigating the spatial distribution of energy consumption. In particular, here we report the visualization of spatial, ATP concentration gradients across cytoskeletal networks, giving insight into how structure, composition and morphology drive energy dissipation.

We use motor-microtubule assemblies as a highly controllable and tunable system due to their minimal components and self-organizing properties in vitro as well as their biological ubiquity. An abundance of work has established that connected dimeric motor domains can cross-link microtubules, creating ordered networks [5, 6, 7, 8]. To control the position, size and start of microtubule cross-linking, we optogenetically link motor proteins together as shown in Figure 2.1, as previously developed in our labs [8]. Motors harness energy to drag microtubules into ordered structures by hydrolyzing an ATP molecule for each step they take along the microtubule. We measure the energy consumed by the motors throughout space and time using a fluorescent, QUEEN-based ATP probe [9] as shown in Figure 2.1.

In addition, to complement the measurements and to provide a framework for understanding them, we develop a reaction-diffusion equation that describes the emergent ATP spatiotemporal gradients and explore the implications of that model with finite element calculations. Combining our experimental and theoretical results, we determine that the measured network formation power is indeed many orders of magnitude greater than the theoretical power of equilibrium processes.

We note that the work presented in the remainder of the paper is written with the

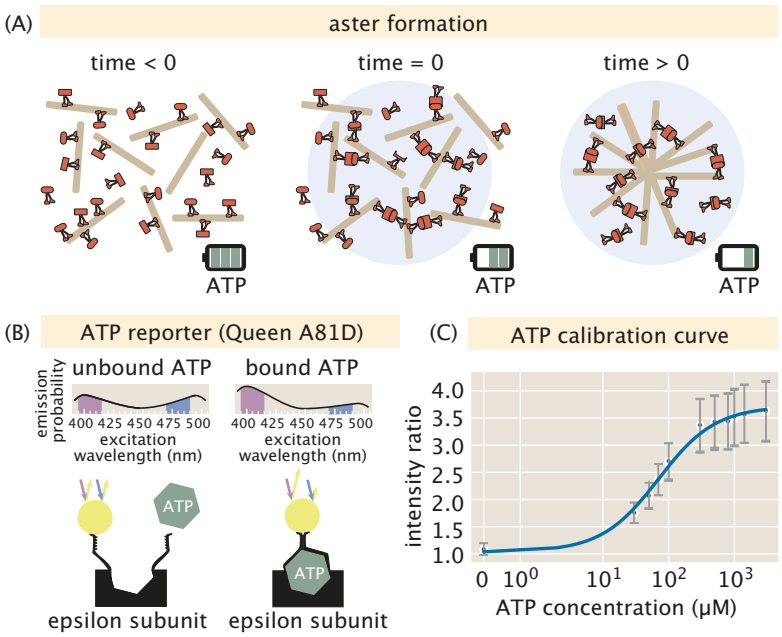

Figure 2.1: **Schematic of the experimental system used to measure spatiotemporal evolution of ATP.** (A) The formation of an aster using light activated motor dimerization. Before light activation, motors independently walk on microtubules hydrolyzing ATP. At $t = 0$ a circular light pattern is projected onto the sample. Motor proteins inside the illuminated region dimerize, crosslinking microtubules. As time elapses, microtubules are dragged into an aster resulting in the depletion of ATP. (B) The binding mechanism for ATP to the ATP probe. Binding ATP to the probe causes the number of emission counts due to an excitation of 405 nm light to increase, while emission counts from 480 nm light excitation decreases. By comparing the ratio of the emission counts at 405 nm and 480 nm light excitations, the concentration of ATP can be inferred. (C) A calibration curve mapping known ATP concentrations to fluorescent light intensity ratios. Each black circle represents the mean ratio value for a given image and gray error bars report the standard deviation of the image.

intention of providing the essential narrative structure in the paper itself. In parallel, the Supplementary Material is written with the aim of making every technical detail of how the experiments were done, how the data was analyzed, how conclusions were drawn and how the data was interpreted using quantitative models completely and rigorously transparent.

2.3 ATP Concentrations in Space and Time

The key elements of our experimental design are shown in Figure 2.1. As noted above, using spatially and temporally controlled illumination, we can generate patterns such as the radially symmetric aster shown in the schematic. Our principal experimental goal is to measure the rate of consumption of ATP as a function of position and time, a goal that is realized by using the fluorescent, ratiometric ATP reporter [9] depicted in Figure 2.1(B). The probe mechanism creates a change in the protonation state [10] of the fluorophore when ATP binds [11], triggering a shift in the fluorophore's absorption spectrum [12]. By using known standards, as shown in Figure 2.1(C), we can construct a calibration curve that now permits us to measure the ATP concentration in a given spatial region. Given that the characteristic scale of ATP concentrations in our experiments are of order 100 μM, we see that our ATP probe can measure ATP consumption in a spatially resolved fashion since, as seen in the calibration curve, the ATP reporter is sensitive in precisely the concentration ranges over which the reporter is effective. Note that in the Supplemental Information, we give an extremely detailed description of how we handled uneven illumination and photobleaching, a prerequisite to a calibration curve like that shown in Figure 2.1(C). In addition, there we also describe how we used two-dimensional images to make approximate three-dimensional inferences.

This measurement scheme equips us to simultaneously resolve the quantity of both ATP and motors over space and time while asters form, as shown for representative time courses in Figs. 2.2(A) and (B). As motors step along and exert torques on microtubules, they accumulate in the centers of assembling asters, creating self-organized polar order and material flow, as witnessed in the time course of Fig. 2.2(A). Concurrently, our measurements report how an initially uniform concentration of ATP is steadily reduced, as shown by Fig. 2.2(B). Importantly, the depletion of ATP is manifestly nonuniform over space, forming a steepening gradient of ATP, with less ATP in the aster center than at its periphery. These concentration fields are displayed as radial profiles in Fig. 2.2(C) and Fig. 2.2(D), registering rich time and space dependencies.

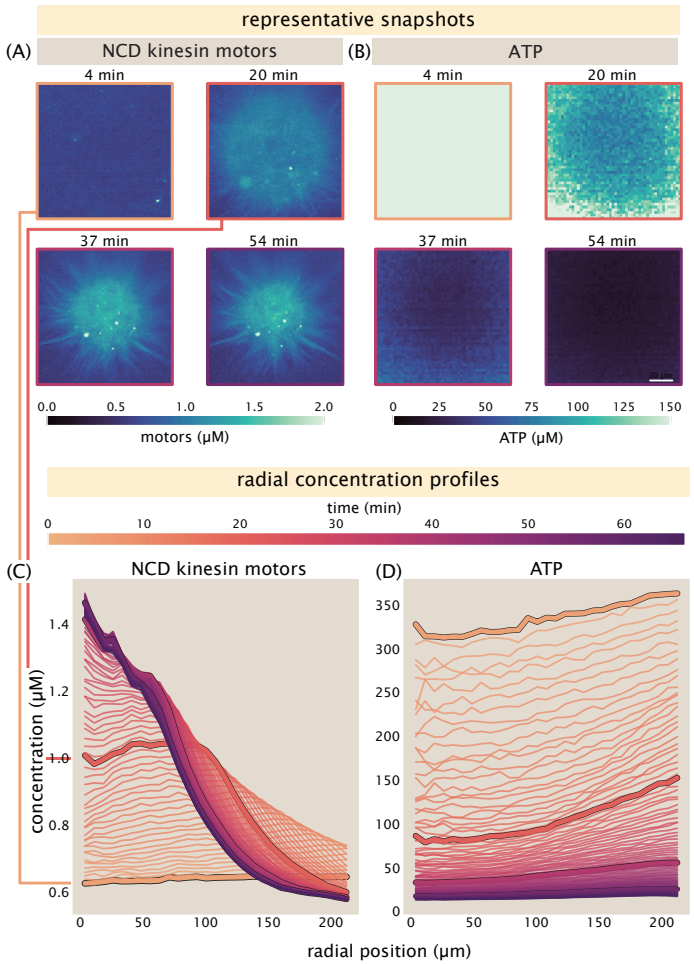

Figure 2.2: **Experimental measurements resolve coupled gradients of motors and ATP across space and time.** (A) Experimentally measured spatial distributions of molecular motors and (B) ATP over four timepoints during the self-organization of an aster. As time evolves, motor proteins concentrate near the aster center; a coupled ATP gradient develops, with greatest depletion in the aster's center where motors are most abundant. (C) Radial concentration profiles of motors and (D) ATP using the same data as in (A) and (B), once angularly averaged, have been highlighted with thick strokes outlined in black at each respective time. These gradients reveal clear, rich nonuniformities over time and space.

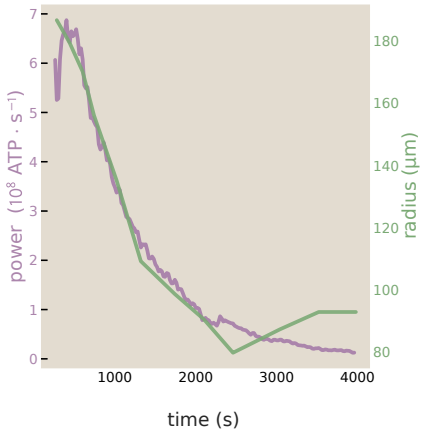

Figure 2.3: **The power of aster formation.** The number of ATPs consumed per second is plotted as a function of time in purple. The green line on top reports the aster radius over time. Under these conditions (0.6 μM motors and 500 μM initial ATP), the magnitude of power tends to follow the size of the aster, consuming ATP faster while first aggressively contracting, and reaching a baseline power level once the aster is no longer dramatically changing size.

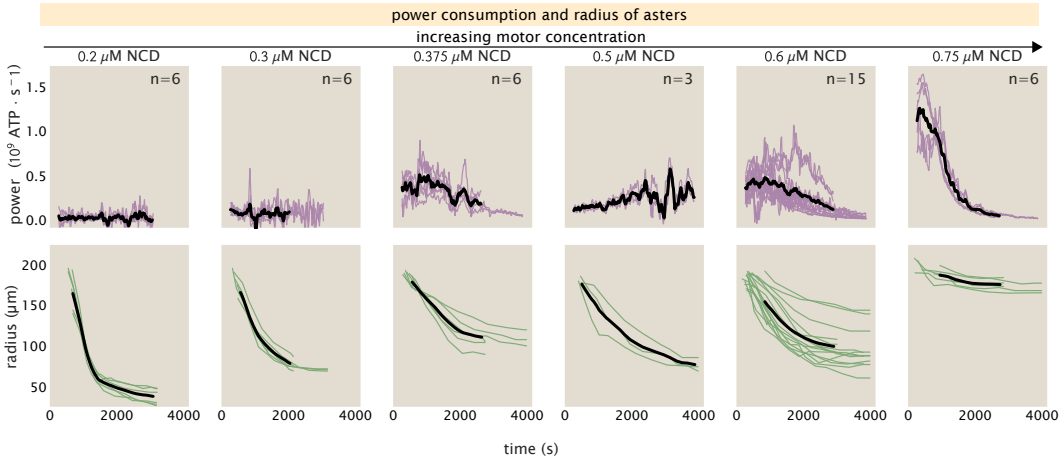

Figure 2.4: **Sizes and power demands of asters across varying motor concentrations.** Top: Measured rates of ATP depletion (top, in purple traces) and characteristic aster sizes (bottom, in green traces) over time across increasing total motor concentrations (as columns from left to right). Distinct experimental replicates are each shown as thin lines to reflect the typical reproducibility of the phenomenonlogy of aster trajectories in each condition, with the number of replicates indicated in the upper right corner. The median trajectories are depicted as black lines. The representative trajectory depicted earlier in Figs. 2.2 and 2.3 is among the trajectories shown in the penultimate (0.6 μM motors) column of this plot.

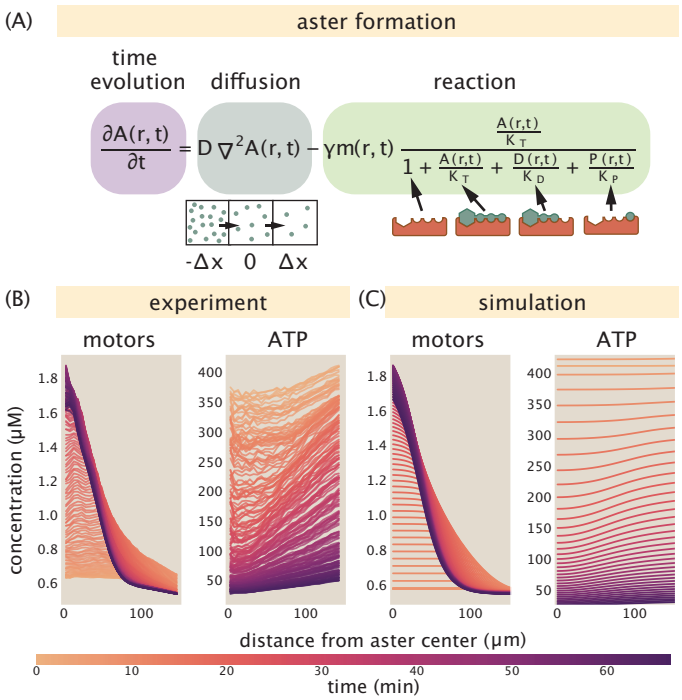

Figure 2.5: **Experimental measurements and Finite Element simulations of ATP concentration in space and time.** (A) The reaction-diffusion equation used to simulate ATP concentration is written with illustrations of the diffusive term and the binding states of ATP (A), ADP (D) and phosphate (P) to the motor protein schematized in red. (B) The radial concentration profile of motors and ATP as measured experimentally. (C) The radial concentration profile of motors and ATP as computed using finite element calculations of a continuum reaction-diffusion equation. As time evolves, motor proteins become concentrated near the aster center while ATP depletes. Both the experiment and simulation reveal an ATP gradient with the greatest depletion in the aster center, where motors are most concentrated.

Another way of visualizing the results of our measurements is to take the ATP data from successive instants and convert it to a power. As shown in Figure 2.3, the power can be evaluated directly in units of ATP/s, making it possible to compare directly to other measurements, as well as estimates of what the energy from hydrolysis events is used to pay for. Next, we ask how one might develop quantitative intuition for the distribution of the ATP in the aster in both space and time.

How do presiding physical parameters, such as the total abundance of motors and initial ATP, control the dissipative and geometric trajectories of asters as they form? To approach this question, we varied the concentration of molecular motors and measured how the rates of ATP depletion over time changed. Across a $\gtrsim$ 3-fold range of sub-micromolar motor concentrations, motors and microtubules varied the

extent to which they macroscopically built prominently recognizable asters over longer than an hour, as visualized by the bottom row of Fig. 2.4 showing aster radii over time. Concomitantly, these structures across motor concentrations shows very different trajectories of power consumption over time, as reported by the power trajectories given by the top row of Fig. 2.4.

These experiments also contribute a measure of the variability attending aster formation, a stochastic process, over biological and technical replicates; individual aster trajectories under repeated conditions are shown as thin lines in Fig. 2.4. While the contraction rates and ATP depletion rates are largely macroscopically reproducible for many total motor concentrations, the reproducibility of these aster formation radial and dissipative trajectories also appeared to vary based on the ambient amount of motors. For instance, we observed particuarly large inter-aster variation at 0.6 μM motors, as shown by the more difergent trajectories of the penultimate column of Fig. 2.4. We note with curiosity that this regime of greater variability appears to be just at the cusp of transitioning from asters that readily contract (giving the appreciable changes to aster radii, at motor concentrations $\lesssim$ 0.6 μM motors) to those that barely macroscopically contract (yielding the only slight changes to aster radii, at motor concentrations $>$ 0.6 μM motors).

The profiles revealed in Figure 2.5 characterize the radial and temporal dependence of both the motors and the ATP. As seen in the dynamical equation in Figure 2.5(A), the change of concentration in some small material volume element can be attributed both to ATP molecules entering and leaving that small region and to the hydrolysis of those ATP molecules by molecular motors that are in the material volume element of interest. More precisely, as shown in the figure, we can write a reaction-diffusion equation that captures the rate of change of ATP in a material volume element. As shown by the box underneath the equation in Figure 2.5(A), a material volume element of interest has molecules both leaving and entering as a result of diffusion, as described in more detail in the Supplement. The reaction term uses a Michaelis-Menten-like dynamics for the rate of ATP consumption by motors. However, the denominator of that term also includes terms that reflect competitive inhibition of the reaction due to ADP and P_i. The local hydrolysis rate is proportional to the density of motors and to the concentration of ATP itself. Note that there is another more pernicious dynamic taking place during our experiments, namely, photobleaching. We have several sections in the Supplemental Information that describe how we measure and account for photobleaching, including thorough finite

element simulations of a diffusion-photobleaching equation in Section 3.8.

One convenient way to analyze the solutions to such equations in diverse geometries is by appealing to numerical methods. In our case, we used the finite element method to compute the space-time history of the ATP as shown in Figure 2.5(C). As seen in the figure, for reasonable parameter choices (the details of parameter selection are described in the Supplement), the time evolution of the ATP field is in reasonable accord with our measurements. One question that naturally arises is to ask what that ATP hydrolysis "pays for?" Of course, mechanistically, we know that the ATPs are being consumed by motors as they carry out their walk along microtubules. But here we mean it differently. That energy is dissipated through elementary processes such as ordering and contraction of the microtubule network. How much energy do these processes cost? Microscopically, a huge variety of dissipative processes are taking place during the microtubule-motor rearrangements attending aster formation. As shown in Figure 2.3 the power varies considerably at different stages of the aster formation process. To that end, we explore the power associated with a variety of processes that we imagine are taking place concurrently and would cost different amounts at different stages of the aster formation process. Indeed, as seen in Figure 2.6 there are a number of possible estimates that one can make in units of ATP/s that reflect what ATP hydrolysis might be used to "pay for." Each of these estimates (and several others) is spelled out in detail in the Supplemental Information in Section 4.2 and here we simply describe the concept of each calculation and how much power consumption it implies.

Given the measured power, we were intrigued to compare it to the power associated with a variety of elementary dissipative processes that take place during aster formation as shown in Figure 2.6. For example, as is evident from the radius as a function of time in Figure 2.3, the volume of the microtubule aster is decreasing over time. As shown in Figure 2.6(A) and described in detail in Section 4.2, we can perform a simple estimate of the power associated with this contraction as the pV work done divided by the elapsed time. We find that the pV power is five orders of magnitude smaller than the measured power. As shown in Figure 2.6(B), a second dissipative process is the frictional sliding of the various microtubules during the contraction process. A naive estimate is obtained by replacing a given microtubule by a corresponding sphere of the same dimensions and to work out the Stokes drag. As in the case of the pV power, this results in a power that is five orders of magnitude smaller than the measured power of Figure 2.3. As discussed

in Section 4.2, a better estimate can be made in which the microtubule is treated as a rod rather than a sphere and in this case the computed power is even smaller. Another approach to estimating the power is offered by field theories of nematic ordering in which the state of the system is characterized by the spatially varying tensor $Q_{ij}(\mathbf{f}, t)$. This estimate is trickier to make since the parameters in such a field theory of motor-microtubule systems are not well known. Nevertheless, as seen in Figure 2.6(C) (and described in more detail in the Supplement), the power we estimate associated with such ordering is many orders of magnitude smaller than the measured power. The final dissipative process highlighted in Figure 2.6(D) is that of maintaining a nonequilibrium gradient of motors radially outward from the center of the aster. One way to think about such a gradient is that if there were not some active transport carrying motors towards the aster center, then diffusion would smooth out that gradient. As we show in Section 4.2, there is a well defined prescription for estimating the power to maintain such a gradient and we find that it is of the same order of magnitude as the measured powers. This interesting result suggests the hypothesis that a significant fraction of the ATP hydrolysis consumed by the motors is "spent" to build and then maintain this gradient.

2.4 Discussion

It is practically a cliche to note that living organisms are "out of equilibrium." But we also find that this compact, binary statement, while true, is largely unhelpful. Equilibrium ideas are even used to describe the conditions in a star, and it behooves us to have quantitative measures of what we mean by the word "nonequilibrium" in different contexts. For example, although a bacterium can be thought of as a furnace burning fuel at a rate of 10^5 W/m^3, for single cells and even embryos, this power consumption leads to a temperature change relative to the external world of less than 10^{-7} K. Though each ATP hydrolysis event leads to a local temperature change of ≈ 10 K in a 1 nm^3 volume, that temperature change relaxes away at time scales far less than a microsecond. Similarly, the concentration gradients of morphogens are very shallow implying that the "out of equilibrium" concentration gradient is barely discernible at the molecular scale. To see this, we imagine discretizing the anterior-posterior axis of the fly embryo into little 1 μm^3 boxes, the measured gradients are so gentle that two adjacent 1 μm^3 boxes near the anterior part of the embryo would have an average of 60 and 59 molecules, respectively. The point here is that the question of the extent to which biological systems depart from equilibrium is both important and subtle.

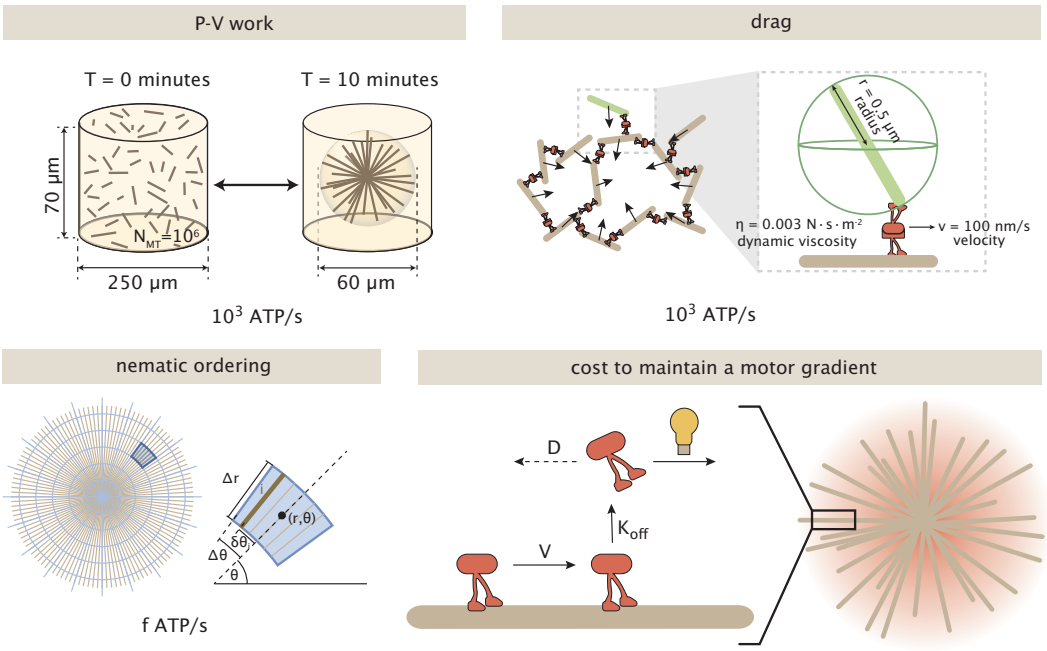

Figure 2.6: **Mechanistic processes taking place during aster formation and their estimated power.** Each schematic considers a different dissipative processes that occurs during the formation of an aster. (A) Schematic of the power of compressing an "ideal gas" of microtubules. (B) The power of dragging microtubules through a viscous medium. (C) Power estimate for inducing nematic ordering in a random array of microtubules. (D) The power to maintain a concentration gradient of motors in the aster.

In recent years, renewed efforts have been made both experimentally and theoretically to explore the deep question of when and where energy is being consumed within cells and what the energy consumption is used for. A seminal study in the 1970s by Stouthammer already recognized the huge energetic burden of protein synthesis in fast growing cells [13]. This process sets a baseline of roughly 10^6ATP/(μm^2 s) because to produce the $\approx$ few $\times\, 10^2$ peptide bonds per protein each of which costs 4 ATP equivalents for the roughly few $\times\, 10^6$ proteins per cell results in a total cost of $\approx$ few $\times\, 10^9$ ATPs over the 1000 seconds of the cell cycle. Recent experiments in bacteria illustrated how in starved cells after roughly 24 hours they die due to a loss of membrane potential. Here too, we can make simple estimates of the power required to maintain the transmembrane potential against membrane leakage. Stated simply, the flux of ions out of the cell can be estimated as $dn/dt = JA$, where $J = p\Delta c$. Using the very low permeability to ions of roughly $p \approx 10^{-9}$ nm/s, we find that the net loss of ions occurs at a rate of 1 - 10 ions/s. Using the relation $\Delta Q = C\Delta V$, we can estimate that in under 24 hours the membrane potential will be

nearly completely lost. The power to maintain the membrane potential against such leakage is a tiny value of 10s of ATPs per second.

We argue that the management of energy expenditure in space and time is of critical importance for understanding everything from the development of membrane potentials to the fidelity of biological polymerization to the assembly of structures such as the spindle. Recently, both calorimetry and fluorescence approaches have made it possible to dissect the dissipation in living cells. Such measurements generally tell a similar story, namely, that the scale of measured dissipation is often orders of magnitude larger than the dissipation one might expect by considering elementary processes such as flow [1].

In this paper, we rigorously measured such energy consumption in space and time in the specific context of a microtubule-motor system. Our measurements resolving large spatially varying power consumptions, understood from a slew of theoretical contexts, provoke immediate questions, both empirically and conceptually.

Empirically, precisely how dramatically do spatial gradients of ATP and ATP consumption rates develop and persist inside whole cells (whether metabolically replete or stressed)? Our work directly quanties the growth and extinguishment of dramatic dissipative gradients from an initial unreplenished ambient ATP pool by a dominant sink process (namely, motors). Whole cells, however, couple the equivalents of these sink processes with metabolic sources (including mitochondria). It is a fascinating, abiding question for our field, whose urgency is sharpened by our work, to ask whether or how the conspiracy of both sources and sinks manifests appreciable gradients (or not) of biochemical sources of energy. Our measurements establish that gradients might be eminently physiologically plausible. Yet, the sustainment and quantitative extent of extant gradients inside cells must be explicitly measured across metabolic conditions to understand the true physiological consequences of such gradients.

Conceptually, if cells spend more energy than they appear to "need" to to accomplish certain key tasks, can explicit spatial readouts of their dissipation reveal other functional priorities that constrain them? Could new control schemes for physiology across organelles be unlocked by such metabolic gradients in space? At the level of fundamental nonequilibrium physics, how can amazing recent theoretical progress in stochastic thermodynamics (e.g., as discussed in [14]), whose results are very frequently spaceless, be updated to incorporate the rich new consequences of spatial effects?

We anticipate rapid fundamental discoveries await these basic questions informed by developing "spatial metabolomics" tools that measure ATP or its equivalents in real units on biologically-relevant length- and time-scales.

References

[1] Peter J. Foster et al. "Dissipation and energy propagation across scales in an active cytoskeletal material." In: *Proceedings of the National Academy of Sciences* 120.14 (2023), e2207662120.

[2] Jonathan Rodenfels, Karla M. Neugebauer, and Jonathon Howard. "Heat oscillations driven by the embryonic cell cycle reveal the energetic costs of signaling." In: *Developmental Cell* 48.5 (2019), pp. 646–658.

[3] Qiwei Yu, Dongliang Zhang, and Yuhai Tu. "Inverse power law scaling of energy dissipation rate in nonequilibrium reaction networks." In: *Physical Review Letters* 126.8 (2021), p. 080601.

[4] Yuansheng Cao et al. "The free-energy cost of accurate biochemical oscillations." In: *Nature Physics* 11.9 (2015), pp. 772–778.

[5] François J. Nédélec et al. "Self-organization of microtubules and motors." In: *Nature* 389.6648 (1997), pp. 305–308.

[6] Thomas Surrey et al. "Physical properties determining self-organization of motors and microtubules." In: *Science* 292.5519 (2001), pp. 1167–1171.

[7] Johanna Roostalu et al. "Determinants of polar versus nematic organization in networks of dynamic microtubules and mitotic motors." In: *Cell* 175.3 (2018), pp. 796–808.

[8] Tyler D. Ross et al. "Controlling organization and forces in active matter through optically defined boundaries." In: *Nature* 572.7768 (2019), pp. 224–229.

[9] Hideyuki Yaginuma and Yasushi Okada. "Live cell imaging of metabolic heterogeneity by quantitative fluorescent ATP indicator protein, QUEEN-37C." In: *BioRxiv* (2021), pp. 2021–10.

[10] Takeharu Nagai et al. "Circularly permuted green fluorescent proteins engineered to sense Ca2+." In: *Proceedings of the National Academy of Sciences* 98.6 (2001), pp. 3197–3202.

[11] Hideyuki Yaginuma et al. "Diversity in ATP concentrations in a single bacterial cell population revealed by quantitative single-cell imaging." In: *Scientific Reports* 4.1 (2014), p. 6522.

[12] Roger Y. Tsien. "The green fluorescent protein." In: *Annual Review of Biochemistry* 67.1 (1998), pp. 509–544.

[13] A. H. Stouthamer. “Theoretical study on amount of ATP required for synthesis of microbial cell material.” In: *Antonie Van Leeuwenhoek Journal of Microbiology* 39.3 (1973), pp. 545–565.

[14] Massimiliano Esposito, Upendra Harbola, and Shaul Mukamel. “Nonequilibrium fluctuations, fluctuation theorems, and counting statistics in quantum systems.” In: *Reviews of Modern Physics* 81.4 (2009), pp. 1665–1702.